Dynamic Compaction of Titanium Aluminides by Explosively Generated Shock Waves: Experimental and Materials Systems

A. FERREIRA, M.A. MEYERS, N.N. THADHANI, S.N. CHANG, and J.R. KOUGH

Different approaches to compact cylinders of titanium aluminide powders by explosively generated shock waves were explored. Two basic compositions of the titanium aluminide powders produced by the rapid solidification rate (RSR) technique were used: Ti-21 wt pct Nb-14 wt pct Al and Ti-30.9 wt pct Al-14.2 wt pct Nb. A double-tube design utilizing a flyer tube was used in all experiments. Experimental parameters that were varied were initial temperature, explosive quantity, and explosive detonation velocity. The major problem encountered with shock consolidation of titanium aluminides was cracking. Titanium aluminide powders were also mechanically blended with niobium powders in one case and elemental mixtures of aluminum and titanium powders in the other case. Enhanced bonding and decreased cracking were observed in both cases. In the former case, the addition of niobium powder provided a ductile binder medium which assisted in consolidation. In the latter case, due to the additional heat generated and melting produced by the shock-induced reactions between Ti and Al, significant improvements in bonding of the titanium aluminide powders were observed.

I. INTRODUCTION

TITANIUM aluminides are potential materials for many of the rotating and static components in the compressor sections of gas turbine engines[1,2] in aerospace applications because of their low density and high-temperature properties.[3,4] The objectives of this work were twofold: (1) to present the macrostructural features resulting from dynamic compaction of rapidly solidified titanium aluminides by explosively generated shock waves and (2) to investigate the effects of alloy composition, niobium powder additions, shock-induced chemical reaction between mechanically blended powder mixtures of titanium and aluminum, initial temperature, amount of explosive, and detonation velocity of the explosive on the cracking density of compacts.

II. EXPERIMENTAL PROCEDURE

A. *Material Characterization*

Table I lists the characteristics (alloy type, run number, composition, pct carbon, and powder size) of the rapidly solidified powders as obtained from Pratt & Whitney, West Palm Springs, FL, and used for the compaction experiments. These powders were produced by the rapid solidification rate (RSR) process. The particle size distribution obtained by sieve analysis was performed at Pratt & Whitney. There is a considerable degree of variation in the compositions reported in Table I. The main differences are in the carbon content and in the presence of erbium for part of the powders. The high-carbon powders (Ti_3Al) are the top four ones in Table I and were solely used for filler material in the containers. For the central portions of the containers, which were subsequently analyzed and tested, the low-carbon powders were used. Erbium additions for a number of runs are intended to improve the high-temperature properties through the formation of erbium oxide.

B. *Experimental Systems*

The experimental setup consisted of two coaxial tubes, the external one being accelerated inward to impact the internal tube that contains the powder. A detailed description of the system is presented elsewhere.[5] The basic experimental system is shown in Figure 1, and this technique is called the flyer-tube or double-tube technique. The explosive charge (an ammonium nitrate-fuel oil (ANFO) mixture with 6 pct oil) is detonated at the top, and a DuPont DETA SHEET* (a 2-mm-thick PETN-based plastic explosive) is used to create a more uniform detonation front. The explosive charge is contained in a polyvinyl chloride (PVC) plastic tube resting on a wood base and surrounds a mild steel flyer tube, in the center of which is the assembly containing the powder (stainless steel pipe with top and bottom steel plugs). The containers are filled with the powder under argon atmosphere. The central axis of the powder container sometimes has a solid rod (mandrel) to eliminate Mach stem formation.[5] Shock consolidation conditions were varied by changing the detonation velocity and amount of explosive.

In order to impart a greater ductility to the starting powders and to bring them closer to the melting point, it was felt that explosive consolidation of preheated powders would be effective. Preheating the powder may induce sufficient ductility into the powders to make them easy to deform and conform along their neighbors during

*DETA SHEET is a trademark of E.I. DuPont de Nemours & Co., Inc., Wilmington, DE.

A. FERREIRA and J.R. KOUGH, Department of Metallurgical and Materials Engineering, and N.N. THADHANI are with the Center for Explosives Technology Research, New Mexico Institute of Mining and Technology, Socorro, NM 87801. M.A. MEYERS and S.N. CHANG are with the Center of Excellence for Advanced Materials, University of California, San Diego, La Jolla, CA 92093.

Manuscript submitted September 5, 1989.

Table I. Characteristics of Ti_3Al and TiAl Powders

Based Alloy	Run	Composition (Wt Pct)	Pct Carbon	Particle Size Distribution Mesh
Ti_3Al	297	Ti-21Nb-14Al-0.75Er	0.151	−325/+ 80
	298	Ti-21Nb-14Al-0.75Er	0.232	−325/+ 80
	301	Ti-21Nb-14Al-0.75Er	0.162	−325/+ 80
	320	Ti-21Nb-14Al	0.199	−200/+ 80
	322	Ti-21Nb-14Al	0.049	−140/+ 80
	346	Ti-21Nb-14Al	0.032	−140/+ 80
	347	Ti-21Nb-14Al	0.080	−140/+ 80
	348	Ti-21Nb-14Al	0.034	−140/+ 80
	357	Ti-21Nb-14Al	0.050	− 80
	398/399	Ti-21Nb-14Al	0.025	—
	444/445/453	Ti-21Nb-14Al-1.0Er	0.016	−325/+ 50
	450	Ti-21Nb-14Al-1.0Er	0.017	−325/+ 80
	446/452	Ti-21Nb-14Al-1.0Er	0.014	—
	471	Ti-21Nb-14Al-1.0Er-1.0B	0.102	−325/+ 50
TiAl	531	Ti-32.6Al-0.81V	0.145	−200/+100
	CYC80	Ti-34.0Al-1.3V	0.195	− 80
	CYC50	Ti-34.0Al-1.3V	0.195	− 50
	1111	Ti-34.0Al-1.3V-2.0B-1.4Er	0.540	− 80
	1113	Ti-34.0Al-1.3V-1.0B	0.240	− 80
	1113	Ti-34.0Al-1.3V-1.0B	0.240	−200
	1115	Ti-34.0Al-0.75B	0.240	− 80
	1117	Ti-34.0Al-1.5B	0.276	− 80
	1160/1161	Ti-30.9Al-14.2Nb-1.1Er-1.1B	0.552	—
	1162	Ti-32.4Al-20.2Nb-1.1Er-1.0B	0.402	−325/+ 50
	1251	Ti-33Al-5Nb-1.0Ta	0.140	−325/+ 50

the consolidation process. Earlier experiments conducted by Wang *et al.*[6] on nickel-base superalloys indicated that preheating to 500 °C to 700 °C had a very positive effect on the mechanical properties of shock-consolidated superalloys. The system developed by Wang *et al.*[6] used a bottom initiation and an armor plate to trap the specimen. A new system, whose basic components are shown in Figure 2, was designed for the specific purposes of this investigation. The sample containing the powder is preheated at different temperatures and rested on top of the push-tube. When the lower solenoid is released, the counterweight comes down and the push-tube is activated; as a result, the sample is lifted to its final position (Figure 2(b)). At this moment, the sample capsule is inside the flyer tube and is surrounded by the explosive. In this condition, the explosive experiment is ready to be initiated (at top). In case of misfire, the upper solenoid is activated and the powder container drops down. The principal advantages of this design over the one by Wang *et al.*[6] are as follows: (a) the initiation is at the top and the system is accelerated downward (thus, an armor plate to trap the sample is not required); and (b) in case of misfire, the capsule can be retrieved from the explosive. This procedure prevents the hot sample from cooling down inside the explosive and, consequently, prevents the risk of accidental detonation.

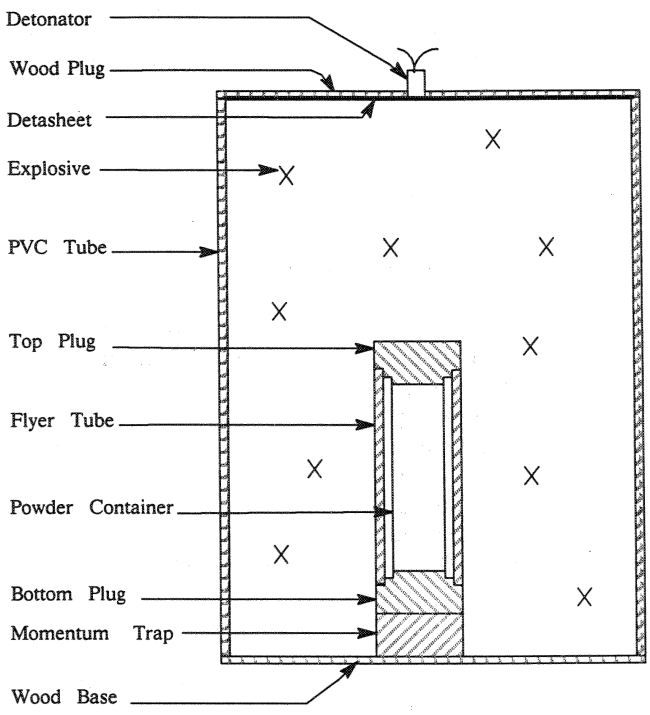

Fig. 1—Cylindrical axisymmetric double-tube system.

The effect of the amount of explosive was investigated by using two different diameters of the explosive container (PVC) tube, ϕ = 150 mm and ϕ = 213 mm, at both ambient and high temperature (600 °C). The influence of the explosive was verified at room temperature using two different types of explosives (ANFO) with detonation velocities equal to 3500 and 2200 m/s. Additional details are given in Section D.

C. *Powders*

Three classes of shock consolidation experiments, in which the powder mixture was varied, were conducted in order to maximize interparticle bonding and minimize

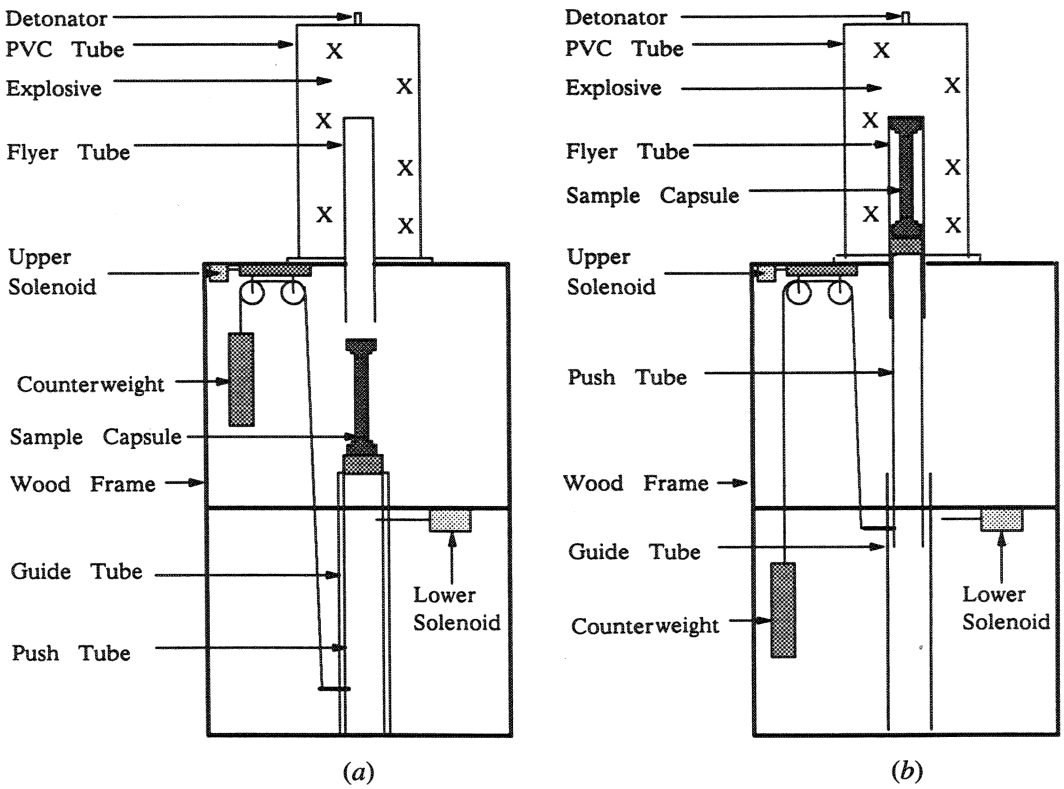

Fig. 2—Schematic view of high-temperature device: (*a*) capsule in initial position and (*b*) capsule in final position.

cracking. In order to obtain good consolidation, it is necessary for the initial shock wave to have sufficient amplitude so that it can deform the particles and collapse all of the initial voids. Figure 3 shows schematically the idealized interparticle bonding intended for the three classes of experiments. Figure 3(a) presents the first case, in which the experiment is carried out with titanium aluminide powder only. Before the shock wave moves through the powder, the particles have a spherical shape (characteristic of the RSR process) and are loosely packed. In the final state, after the passage of the shock wave, the particles are deformed and a layer of molten and resolidified material surrounds them, thus providing a strong interparticle bonding among them. Figure 3(b) shows the situation in which the titanium aluminide powder is blended with niobium. In this case, the niobium particles will be deformed more intensely than the titanium aluminide particles (because of the lower yield stress of Nb) during the propagation of the shock wave and they help to provide bonding among the titanium aluminide particles. The disadvantage of adding niobium resides in its high density (8.59 g/cm^3); the addition of 15 wt pct Nb increases the density of Ti_3Al and TiAl by 10.7 and 16.8 pct, respectively. Niobium was added to enhance the ductility of the final product by acting as a ductile constituent. Figure 3(c) shows the use of elemental powders (Ti and Al) blended with inert intermetallic powders (Ti_3Al and TiAl). The passage of the shock wave activates highly exothermic reactions between Ti and Al that provide enhanced bonding between the inert intermetallic powders.

Quantitative determination of cracking was made by taking photographs from the radial sections of the recovered compacts at a magnification of 10 times. Macrocrack measurements were then made from the photographs using the line intercept method. The scatter in the values of macrocrack surface area per unit volume (S_v), measured in cm^2/cm^3, was obtained by cutting three slices

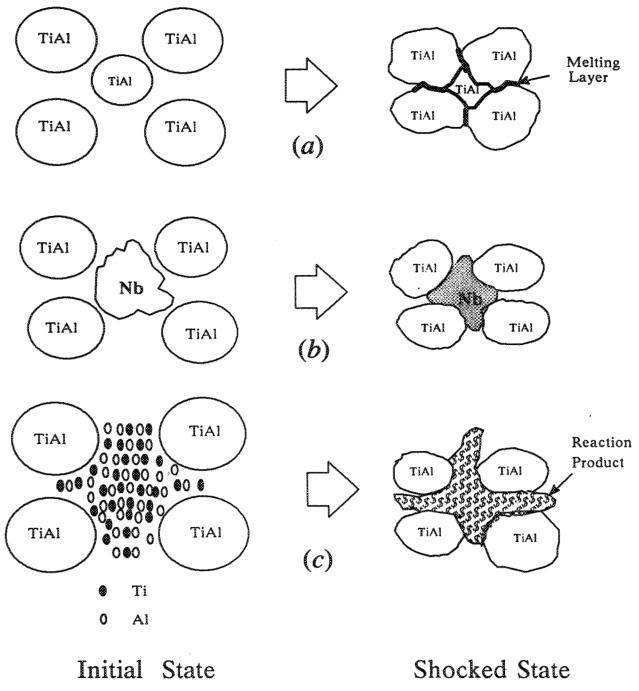

Fig. 3—Schematic interparticle bonding model caused by shock wave: (*a*) titanium aluminide particles; (*b*) titanium aluminide particles blended with Nb; and (*c*) titanium aluminide particles blended with Ti and Al.

of the compacted material and by computing the crack density of each surface separately. This procedure was used for both Ti_3Al- and TiAl-based alloy compacts for experiments performed at room temperature, high temperature, and with the shock-induced reaction-assisted bonding technique.

D. *Calculation of Shock-Induced Pressures*

In order to obtain an understanding of the shock consolidation of Ti-Al intermetallic powders, calculations were made using the Rankine-Hugoniot equations for porous materials. The parameters necessary to calculate the equations of state for Ti_3Al and TiAl powders are reported in Table II. The values determined for Ti_3Al and TiAl solid alloys were obtained assuming that these alloys are a simple mixture (without chemical interactions of the constituents) and that the Grüneisen constant (Γ) is proportional to the specific volume ($\Gamma_0/V_0 = \Gamma/V$). The values of the Hugoniot (C, S) and Grüneisen (Γ) constants for the constituent materials (Ti, Al, and Nb) were obtained by the procedure described by McQueen *et al.*[7] The values of C and S for the solid titanium aluminides were calculated from

$$C = \Sigma\, a_i C_i \qquad [1]$$

$$S = \Sigma\, a_i S_i \qquad [2]$$

where a_i is the atomic fraction of each element in the alloy and C_i and S_i are the Hugoniot constants of each element in the alloy. The plots of Figure 5 actually use weighted averages based on mass fractions of the constituent elements. Table II gives both atomic-based and mass-based calculated values for C and S. The differences are very small (~5 pct). With help from the Rankine-Hugoniot equations for solid and powder, the following relationships can be obtained: pressure *vs* particle velocity, pressure *vs* specific volume, and pressure *vs* specific energy. The procedure is described in detail by Meyers and Wang.[5] Figure 4 shows the pressure *vs* specific volume ratio plots for Ti_3Al and TiAl powders obtained for different initial distensions. Figure 5 shows the pressure *vs* particle velocity for both Ti_3Al and TiAl powders for several packing densities. From the pressure *vs* particle velocity plot, the one-dimensional shock pressure in the powder resulting from metal impacting the powder can be determined using the impedance matching technique after calculating the impacting velocity of the flyer tube. It is given by the intersection point of the transmission Hugoniot of the powder material and the reflected Hugoniot of the metal.

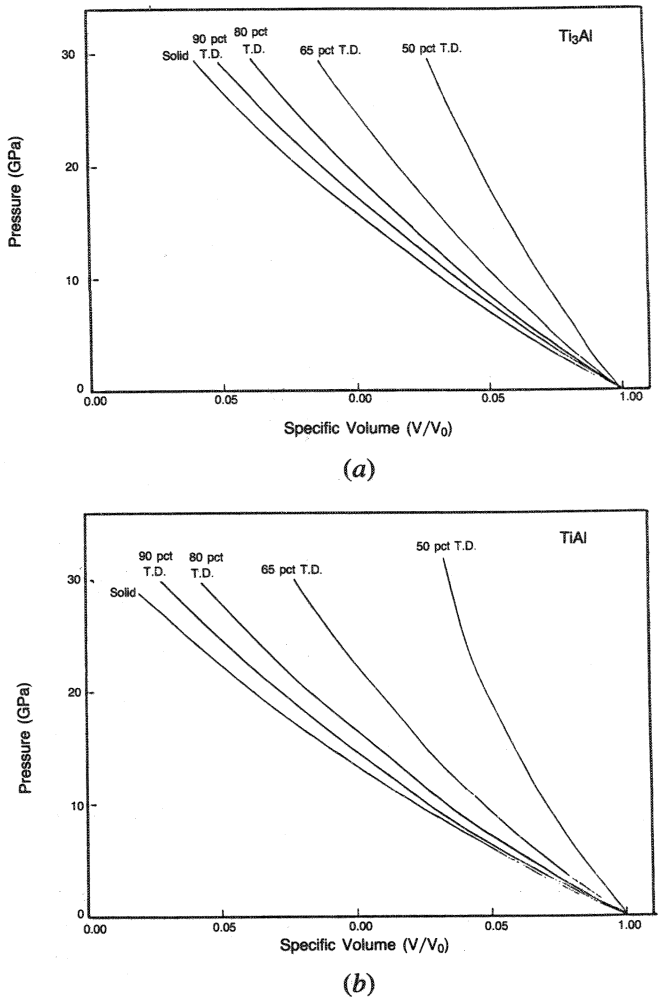

Fig. 4—Pressure *vs* specific volume ratio plot at different packing densities for (*a*) Ti_3Al and (*b*) TiAl.

To obtain optimal compacts, the loading configuration and quantity of explosive have to be determined experimentally. In order to understand better the process of shock consolidation, the flyer-tube velocity was determined by two different methods. In the first one, the flyer-tube velocity was calculated using the modified Gurney equation.[5] Commercially available ANFO-6 wt pct fuel oil was used as the explosive charge. The explosive charge diameter was 216 mm for all experiments except 34, 35, and 37. The charge diameter was 150 mm for the latter. The length of the explosive column was 635 mm. The diameters of 150 and 216 mm are above

Table II. Shock Hugoniot Parameters for Ti_3Al, TiAl, and Their Constituents

Constituent	Γ	Density (kg/m^3)	C (m/s)	S
Ti	1.090	4528	5220	0.767
Al	2.000	2785	5328	1.338
Nb	1.470	8590	4438	1.207
Ti-14Al-21Nb (solid Ti_3Al)	1.122	5137	5162 (at. pct) 5071 (mol pct)	0.956 (at. pct) 0.939 (mol pct)
Ti-30.9Al-14.2Nb (solid TiAl)	1.231	4566	5252 (at. pct) 5142 (mol pct)	1.077 (at. pct) 1.006 (mol pct)

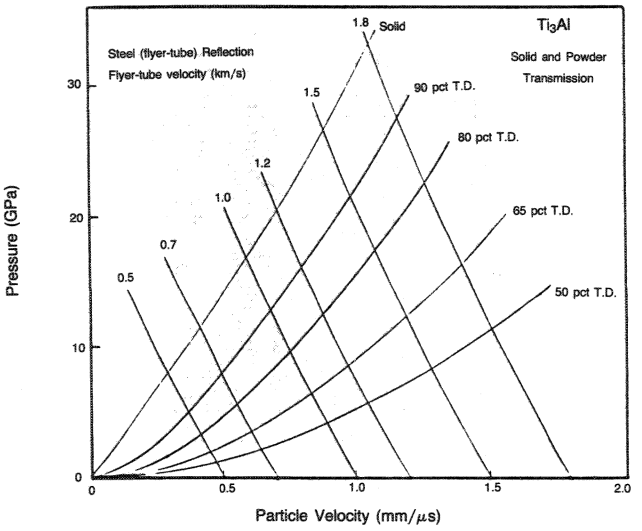

(*a*)

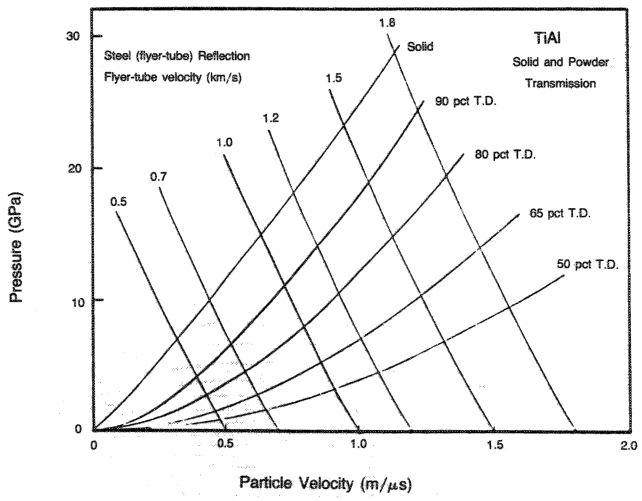

(*b*)

Fig. 5—Pressure *vs* particle velocity plot at different packing densities for (*a*) Ti_3Al and (*b*) TiAl.

the critical diameter for detonation of ANFO. The explosive requires a certain propagation length (approximately equal to its diameter) to reach the steady-state velocity, and this is the reason that the heights of the explosive columns are considerably greater than that of the cylinder containing the powder. The detonation velocity was approximately equal to 3500 m/s. This is lower than the ideal detonation velocity for ANFO (~4900 m/s). For experiments 38 and 39, a lower detonation velocity was obtained by the use of sand added to ANFO. The values $\gamma = 2.8$ and $\rho_c = 0.88$ g/cm^3 for the explosive charge were used. Low-carbon steel was used as flyer tube ($\rho = 7.896$ g/cm^3). By substituting these data in the modified Gurney equation,[5] the value of flyer-tube velocity was determined as 1930 m/s (with the 216 mm diameter charge); with the help of Figure 5, the initial pressures for 65 pct packing density are found to be equal to 18 and 15 GPa for Ti_3Al and TiAl, respectively.

Another way to estimate the flyer-tube velocity is through a computational code. These calculations were conducted by Wilkins[8] using a hydrodynamic, elasto-magneto plastic (HEMP), a two-dimensional (2-D) finite difference code. Figure 6 shows a computer simulation of the 2-D deformation in a cylindrical geometry for the double-tube system at different times. From this figure, one can calculate the flyer-tube velocity as shown below:

$$V_f = U_d \tan \theta \qquad [3]$$

where U_d is the detonation velocity of the explosive and θ is the angle between the flyer tube and powder container. In this computer simulation, the detonation velocity was considered constant and equal to 3500 m/s. The angle θ was measured in Figures 6(b) through (d), and the average flyer-tube velocity was determined as 810 m/s. From Figure 5 and with the value of the flyer-tube velocity previously obtained, the initial pressures generated in the powders were obtained as 4.2 GPa and 3.4 GPa for Ti_3Al and TiAl, respectively. It should be noted that the flyer-tube velocity predicted by a HEMP code was approximately 60 pct lower than the one predicted by the modified Gurney equation. In order to clear these discrepancies, instrumented experiments have to be conducted so that the actual values of the tube-collapse velocity and pressure can be determined.

III. RESULTS AND DISCUSSION

A. *Macroscopic Features in Recovered Compacts*

Macrophotographs of the longitudinal sections of the central portion of some compacts are shown in Figures 7 and 8 for Ti_3Al and TiAl alloys, respectively. Although the compacts appear to be fully densified, cracking does occur, especially in the compacts of TiAl powders. The Ti_3Al powders exhibit much greater ductility (microhardness 400 kg/mm^2) than the TiAl powders (microhardness 500 to 600 kg/mm^2); for this reason, the Ti_3Al compacts show a lesser degree of cracking. Nevertheless, they are both intermetallics and, therefore, inherently brittle. Niobium was added to Ti_3Al to enhance its ductility through retention by rapid solidification of a cubic high-temperature phase. It should be noted that cracking in both Ti_3Al and TiAl powder compacts is a consequence of reflected tensile waves or thermal stresses and is not due to the lack of good bonding between particles. Figures 9(a) and (b) show optical micrographs taken from Ti_3Al and TiAl + Nb compacts, respectively. One can note the transgranular cracks in the compacts (shown by arrows), indicating good interparticle bonding. The white regions in Figure 9(b) are Nb particles that help to provide bonding among the TiAl particles in agreement with the idealized model shown in Figure 3.

The majority of the cracks in the Ti_3Al compacts were normal to the cylinder axis; some of these were caused by the loading of cylinders with different powders. These interfaces gave rise to the lateral cracks shown in Figures 7(a) and (b). These cracks are believed to occur because the tensile strength of the cylindrical compacts is not sufficient to accommodate the tensile longitudinal stresses produced when the shock waves reflect at the bottom of the cylinder. Some lateral and spiral cracks

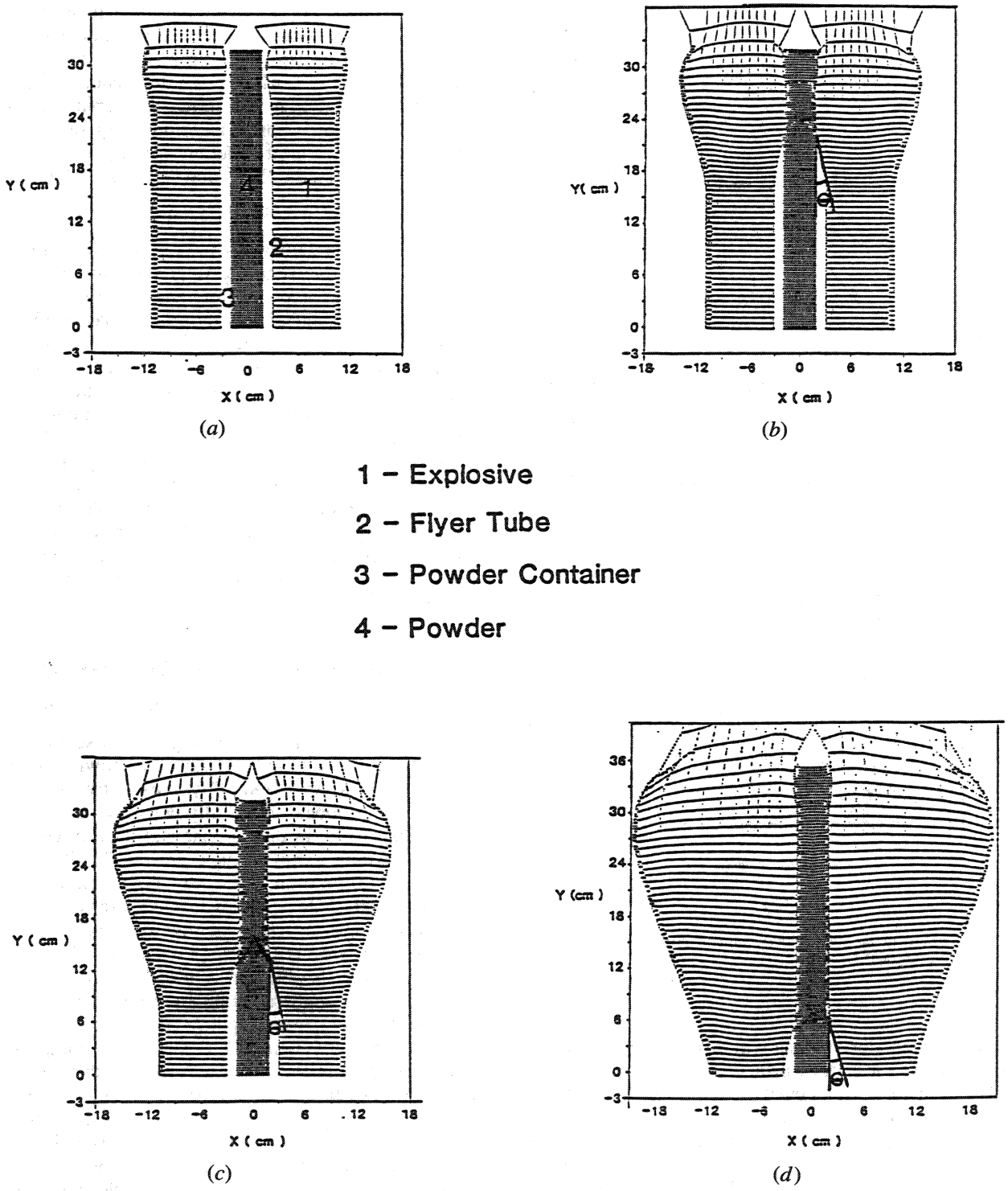

Fig. 6—Computer simulation of shock wave in Ti_3Al powder in double-tube system at different times (courtesy of M.L. Wilkins, Lawrence Livermore National Laboratory, Livermore, CA): (*a*) 25.4 μs, (*b*) 50.8 μs, (*c*) 76.2 μs, and (*d*) 101.6 μs.

are also observed (Figure 7(d)). These cracks result from compressive stresses during loading and tensile stresses during unloading of the shock waves. The materials used for the central mandrel (Al, Ti, and steel) did not appear to show significant effects on the compacts. Figure 7(a) shows an example of a compact using a mandrel of Al, whereas Figures 7(c) and (d) exhibit compacts in which a mandrel of Ti was used. Experiments performed without the mandrel (Figure 7(b)) showed the same degree of compaction and cracking.

The principal type of cracks found in TiAl compacts was spiral (or helicoidal) running at 45 deg to the cylindrical axis. Figure 8(b) shows a typical example of this kind of crack. Spiral cracking is the most severe form of cracking in the cylindrical geometry. In the shock-consolidation process, densification progresses from the

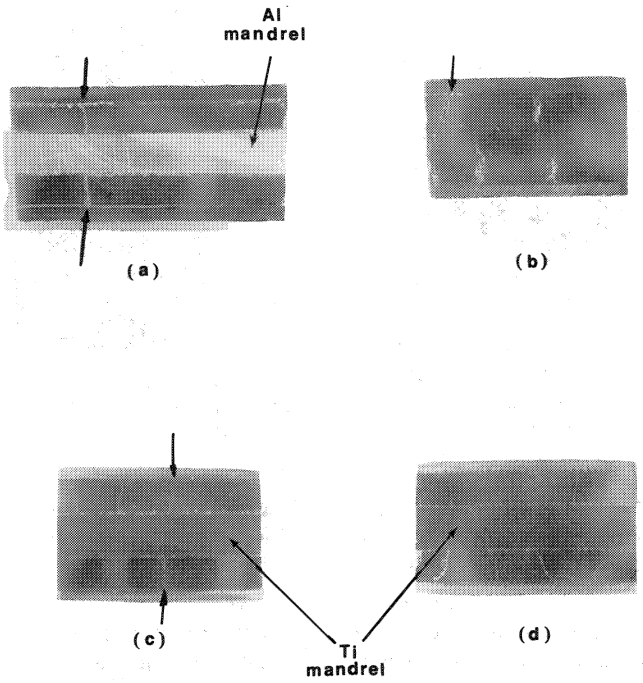

Fig. 7—(*a*) through (*d*) Macrophotographs of longitudinal sections of middle pieces of Ti_3Al compacts.

outer surface of the cylinder toward the central axis. The outer portion of the compact which densifies first must continue to move inward to accommodate for the densification of the inner portion of the compact. If the densified material is brittle, it does not have enough plasticity to deform under the state of stress. As a result, cracks are formed along planes of maximum compressive shear stress. These shear cracks spiral inward to the center and along the axial length of the cylinder. A detailed explanation of cracks and flaws encountered in shock-consolidated cylinders is given by Meyers and Wang.[5] One can find a similar crack formation in static experiments performed by Scholz *et al.*[9] In these experiments, a fully jacketed ring of pyrex glass was tightly fitted over a polished and hardened steel rod. When the ring was subjected to overall hydrostatic pressure, isolated axial cracks were initiated by tiny flaws from the glass interior and grew in a stable manner for long distances.

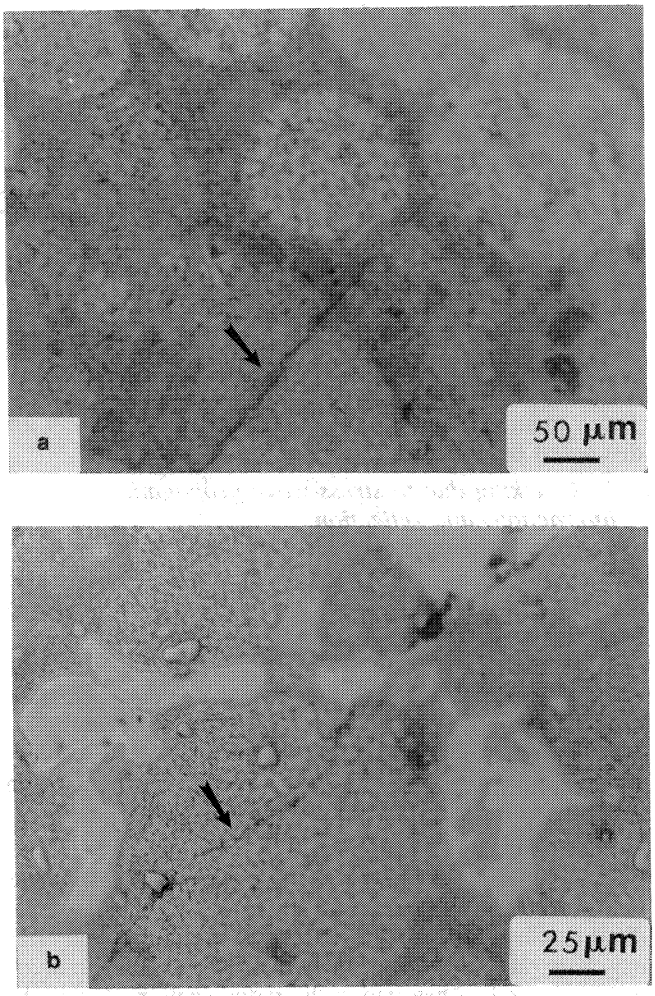

Fig. 9—Optical micrographs from compacts showing transgranular crack which indicates good interparticle bonding: (*a*) Ti_3Al-based alloy and (*b*) TiAl + Nb-based alloy.

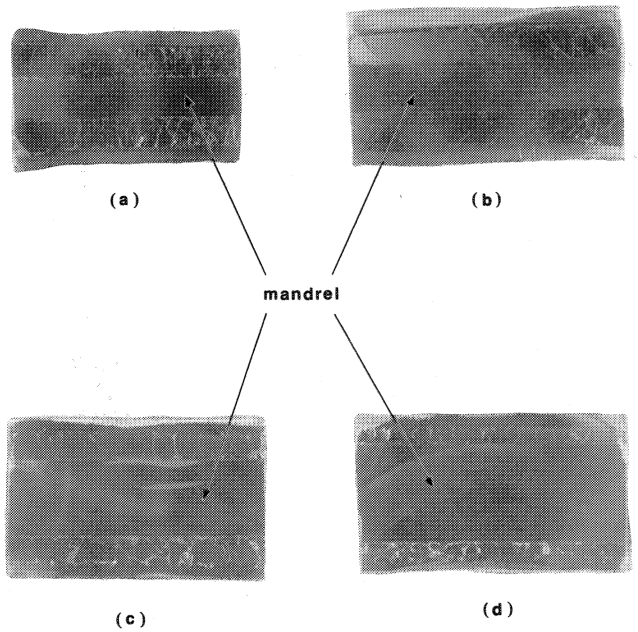

Fig. 8—(*a*) through (*d*) Macrophotographs of longitudinal sections of middle pieces of TiAl compacts.

Figure 8 shows macrographs of longitudinal sections of middle pieces of TiAl compacts and reveals different types of cracks. The effect of loading of layers of dissimilar powders can be seen in Figure 8(a). A batch of 100 gm of low-carbon content powder was loaded in the midsection of the powder container, and the ends were filled with a high-carbon content powder. Figures 8(c) and (d) show the effects of increasing the diameter of the central mandrel. By comparing Figures 8(a) and (b), one sees that cracks in compacts of increased mandrel diameter are spaced further apart.

It was not possible to produce crack-free compacts of either Ti_3Al or TiAl with the double-tube geometry (with or without mandrel) because of the low ductility of the

titanium aluminide powders. Intermetallic compounds are known to be very brittle, and this has been a great technological barrier to their implementation. Nevertheless, the addition of niobium and the retention of the high-temperature disordered β phase enhance the ductility of Ti_3Al and render it workable. Thus, other approaches to reducing cracking were attempted. Through these, it was possible to reduce the incidence of cracking in recovered alloy compacts, although no completely crack-free compacts could be produced. The results of these experiments that present the measured macrocrack density (S_v) are shown in Table III. One can note that the new methods introduced, which involved addition of pure elements, resulted in a considerable decrease in crack density. Three main sources of cracking were identified and are discussed below.

1. *Cracking due to stress-wave propagation, interaction, and reflection*

Figure 10 shows macrophotographs of radial and longitudinal sections of TiAl alloy powder shock compacted after heating to 750 °C, in which transverse cracks are present. The crack density at the outside of the cylinder is much higher than that inside, indicating that all tensile cracks are initiated due to release waves generated from the free surface of the cylinder. Figure 11 shows the radial section of compacted Ti_3Al + Ti + Al alloy powder, in which a circumferential crack is present, resulting from the reflection of the radially expanding compressive wave at the external walls of the cylinder.[5]

2. *Cracking due to embrittling phase transformation*

Figure 12 shows macrocracks on radial and longitudinal sections of the Ti_3Al alloy powder compacted after exposure at 600 °C for 30 minutes. Profuse macrocracking can be observed in the radial section. The high-temperature consolidation experiments with Ti_3Al yielded a significant increase in cracking. The embrittling mechanism is not completely known yet but is being investigated. Preliminary evidence suggests that preheating of the powder transforms the ductile (metastable) β phase into a more brittle α_2 phase, which may lead to the increased cracking in the preheated powders.

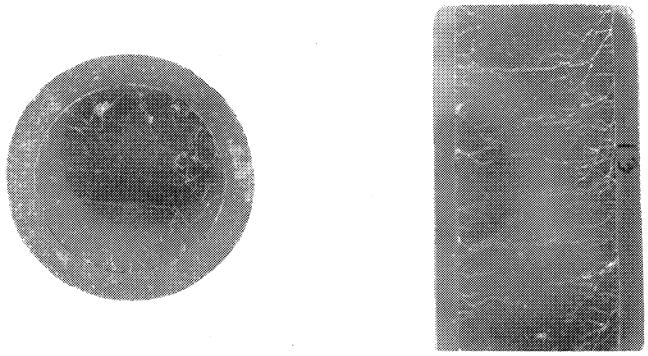

Fig. 10—Macrophotographs of transverse and longitudinal sections of TiAl compacted at high temperature (750 °C), in which transverse cracks due to reflected tensile pulse are present.

3. *Cracking due to thermal stress*

This type of cracking occurs during the cooling of the compacts from the shocked to the ambient state. The shock-consolidated material can reach considerably high mean bulk temperatures during the consolidation process,[10] resulting in residual stresses. Differences in temperature between the specimen core and outside during cooling can accentuate the residual stress and activate the flaws in the material. Figure 13 shows the longitudinal section of the compacted Ti_3Al + Ti + Al alloy powder, in which parallel lateral cracks are present. These lateral cracks may have been induced by thermal stresses.

B. *Effect of Composition*

The effect of composition on cracking of the compacted material is shown in Figure 14 which shows the average macrocrack density occurring in different compositions at room temperature, high temperature

Table III. Values of Macrocrack Surface Area Per Unit Volume (S_v)

Experiment	Alloy Ti_3Al + Ti + Al	S_v (cm^2/cm^3)	Standard Deviation (cm^2/cm^3)	Note
21	Ti_3Al	1.09	0.55	RT
22	Ti_3Al + Nb	0.68	0.17	RT
23	TiAl	5.28	0.15	RT
24	TiAl + Nb	1.67	0.57	RT
28	TiAl + Nb	2.24	0.26	600 °C
29	Ti_3Al + Ti + Al	0.89	0.24	RT
30	TiAl + Ti + Al	1.85	0.45	RT
31	Ti_3Al	2.56	1.34	600 °C
32	TiAl	3.85	0.91	750 °C
33	TiAl	4.98	1.00	600 °C
34*	TiAl + Nb	1.82	0.53	900 °C
35*	TiAl + Nb	2.70	0.13	RT
36	Ti_3Al + Ti + Nb	0.68	0.15	RT
37*	Ti_3Al + Ti + Al	1.38	0.26	RT
38†	Ti_3Al + Nb	0.99	0.05	RT
39†	Ti_3Al + Ti + Al	0.50	0.12	—

*PVC tube with 150-mm diameter.
†Explosive with low-detonation velocity.
RT = room temperature.

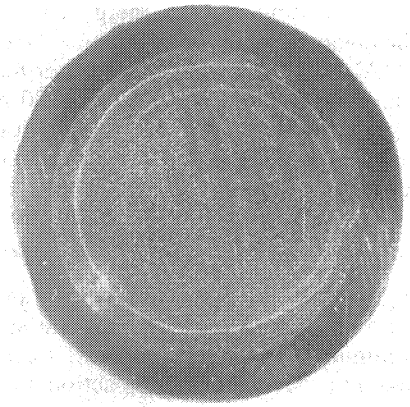

Fig. 11—Macrophotograph of transverse section of compacted Ti_3Al + Ti + Al showing circumferential crack.

(600 °C), and using a low-detonation velocity explosive. At room temperature, cracking occurs more significantly in TiAl-based alloys than in Ti_3Al-based alloys. The best results were obtained with shock-induced chemical reaction-assisted experiments (Ti_3Al + Ti + Al) and with additions of niobium. At high temperatures, the effect of embrittlement due to phase transformations can be observed in the case of Ti_3Al alloy powder which presented more cracks than the TiAl + Nb alloy powder, although the TiAl-based alloy is harder and more brittle than the Ti_3Al-based alloy. The effect of the detonation velocity of the explosive is very clear; in both cases (Ti_3Al + Ti + Al and Ti_3Al + Nb), using the reduced detonation velocity resulted in low crack density. The chemical reaction-assisted shock compacted specimens (Ti_3Al + Ti + Al) presented the best results, exhibiting the lowest value of crack density. This was especially so when the explosive with low-detonation velocity was used. The effect of niobium additions is illustrated in Figure 15. It can be observed clearly that Nb helped to decrease the crack density in the compacted material. Significant improvement was achieved in the case of the TiAl-based alloy for both ambient and high-temperature (600 °C) experiments.

C. *Effect of Initial Temperature*

Figure 16 shows the average macrocrack density of the alloys compacted at various preheating temperatures:

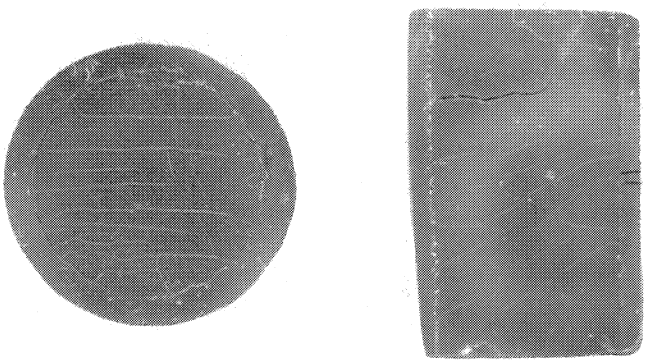

Fig. 12—Macrophotographs of transverse and longitudinal sections of Ti_3Al compacted after exposure at 600 °C showing macrocracks resultant of embrittlement due to high-temperature oxidation.

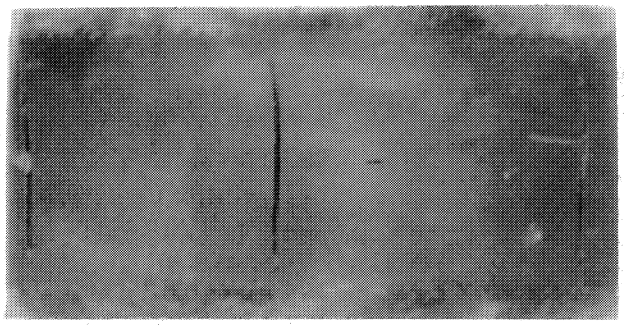

Fig. 13—Macrophotograph of longitudinal section of compacted Ti_3Al + Ti + Al, in which lateral cracks appear to be induced by thermal stress.

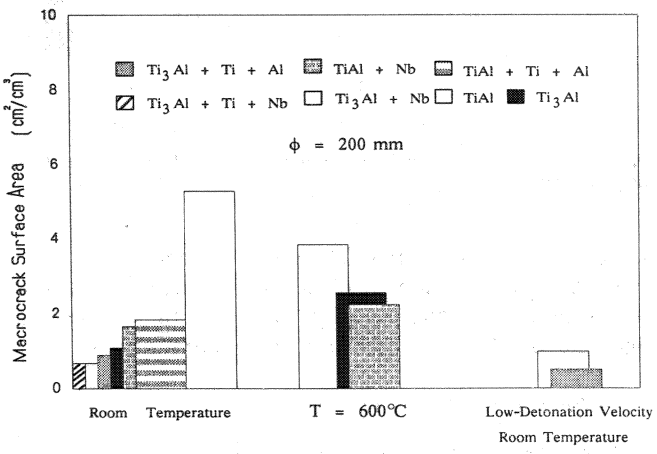

Fig. 14—Effect of composition on the average crack density of compacts.

600 °C, 750 °C, and 900 °C. The preheat consolidations on TiAl alloys were not significantly helpful for reducing the crack density whether or not Nb powder was added. The high initial temperature should provide some degree of ductility to the brittle powders, resulting in a

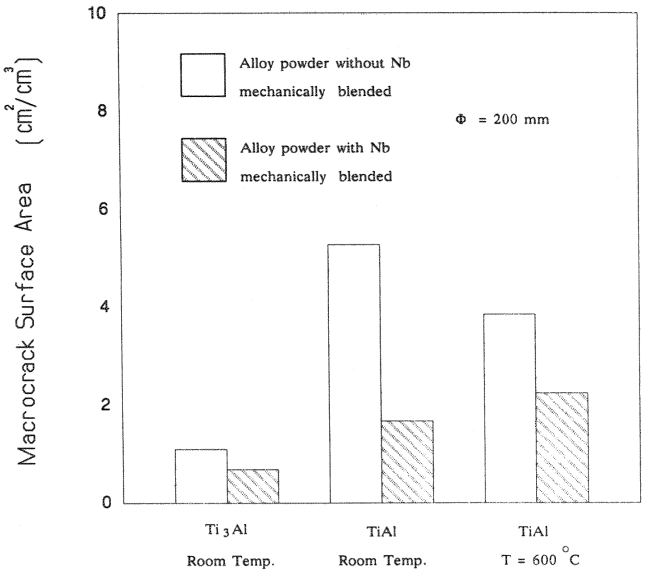

Fig. 15—Effect of niobium additions on the average crack density of compacts.

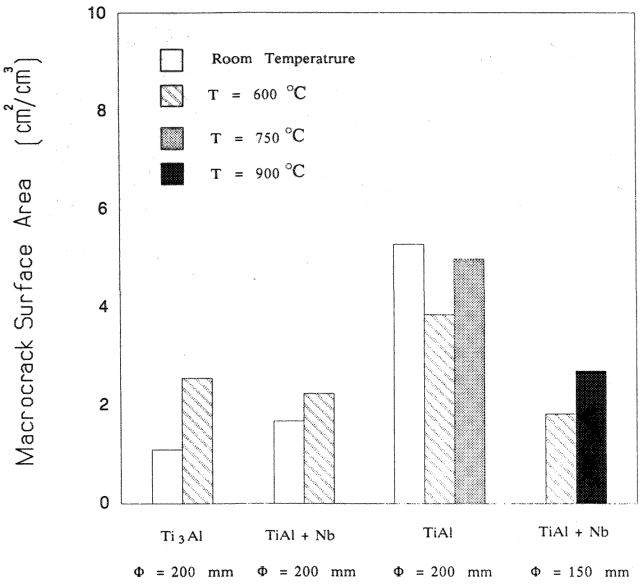

Fig. 16—Effect of initial temperature on the average crack density of compacts.

lesser degree of cracking. The embrittlement of the starting alloy powder due to phase transformations at high temperatures is being investigated, and a microstructural analysis will be presented in a subsequent article.

D. *Effect of Explosive Quantity*

The effect of experimental configuration was investigated both at room and high (600 °C) temperatures, using the same type of explosive in PVC tubes with internal diameters of 150 and 200 mm. The room-temperature experiments for chemical reaction-assisted compaction (Ti_3Al + Ti + Al alloy powder) showed that the larger quantity of explosive helps to reduce cracking (Figure 17). Indeed, the recovered specimen shock compacted in a 150-mm-diameter PVC pipe was underconsolidated, indicating that the energy was not enough to trigger the chemical reaction completely. At high temperatures (TiAl + Nb alloy powder), better results were obtained using the configuration with a 150-mm diameter. At high temperatures, the configuration using a 200-mm diameter may have had excessive energy, resulting in overcompaction of the material.

E. *Effect of Detonation Velocity of the Explosive*

According to Staver[11] and Prümmer,[12] an explosive has to be chosen with detonation pressure sufficient to achieve maximum density in compacts. Excessive detonation pressure produces overcompaction and results in flaws and cracks, whereas low-detonation pressure results in undercompaction and the compacts do not achieve full densification. There are three principal effects (on the compact) of reducing the detonation velocity: (1) the Gurney energy of the explosive is decreased, with a concomitant decrease in the pressure generated in the powder; (2) the angle of incidence of the shock wave in the cylinder is changed; (3) there is a decrease in the amplitude of the reflected waves. The influence of the detonation velocity of the explosive on the average crack density is shown in Figure 18 for the chemically assisted reaction (Ti_3Al + Ti + Al alloy powder) and for the Ti_3Al + Nb alloy which had presented the best results at room temperature (Figure 14). The low-detonation velocity test on the Ti_3Al + Ti + Al alloy was the most effective, reducing the crack density by approximately 40 pct. The delivered energy was sufficient to start the chemical reaction and to compact the powders. The Ti_3Al + Nb alloy did not show any improvement, and the crack density in the compacts was almost the same at both detonation velocities. However, poor interparticle bonding was obtained using an explosive with low-detonation velocity (2200 m/s) as compared to the compacts produced using an explosive with high-detonation velocity (3500 m/s.).

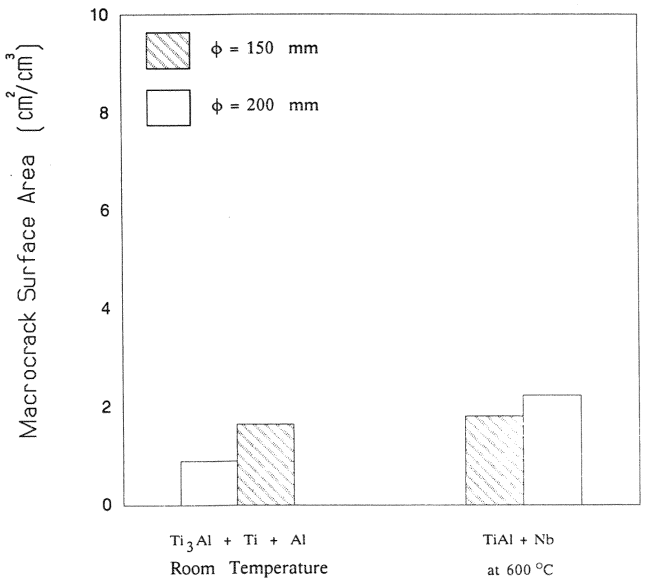

Fig. 17—Effect of amount of explosive on the average crack density of compacts.

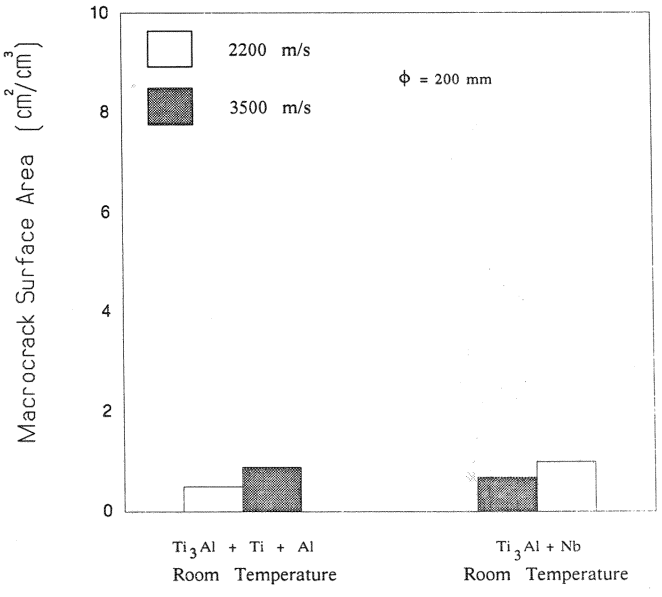

Fig. 18—Effect of detonation velocity of the explosive on the average crack density of compacts.

IV. CONCLUSIONS

Dynamic compaction of rapidly solidified titanium aluminides by explosively generated shock waves could become a viable technique if cracking of the compacts (the main unresolved problem common to the shock consolidation of hard and brittle materials) could be eliminated. The high-temperature experiments, in which the powders were preheated prior to the shock compaction, did not show any significant improvements to reduce the macrocracks in compacted titanium aluminide alloy powders. Furthermore, additional investigation is necessary to determine the source of embrittlement of Ti_3Al alloy powders at high temperatures. Additions of Nb and Ti and Al powders helped to obtain improved compacts for both Ti_3Al and TiAl alloy powders. The shock-induced chemical reaction seems to have considerable potential and should be explored further.

ACKNOWLEDGMENTS

This research was sponsored by Pratt & Whitney Government Products Division. The authors would like to thank Ms. Sandy Shuleshko for her assistance during the work. Dr. M.L. Wilkins carried out the computational simulation and his kind help is greatly appreciated. The CETR Eagle site firing group, Mr. Phil Anthony, Tom Gould, and John LeBarge conducted the shock-consolidation experiments and helped to develop the high-temperature systems; their dedicated collaboration was an important part of this investigation.

REFERENCES

1. D. Shechtman, M.J. Blackburn, and H.A. Lipsitt: *Metall. Trans. A*, 1974, vol. 5A, pp. 1373-81.
2. Harry A. Lipsitt, D. Shechtman, and Robert E. Schafrik: *Metall. Trans. A*, 1975, vol. 6A, pp. 1991-96.
3. Robert E. Schafrik: *Metall. Trans. A*, 1977, vol. 8A, pp. 1003-06.
4. H.A. Lipsitt, D. Shechtman, and R.E. Schafrik: *Metall. Trans. A*, 1980, vol. 11A, pp. 1369-75.
5. M.A. Meyers and S.L. Wang: *Acta Metall.*, 1988, vol. 36 (4), pp. 925-36.
6. S.L. Wang, M.A. Meyers, and A. Szecket: *J. Mater. Sci.*, 1988, vol. 5, pp. 1786-96.
7. R.G. McQueen, S.P. Marsh, J.W. Taylor, J.N. Fritz, and W.J. Carter: in *High Velocity Impact Phenomena*, R. Kinslow, ed., Academic Press, Inc., New York, NY, 1970, pp. 293-417.
8. M.L. Wilkins: Lawrence Livermore National Laboratory, Livermore, CA, private communication, 1988.
9. C.H. Scholz, G. Boitnott, and S. Nemat-Nasser: *Pur. Appl. Geophys.*, 1986, vol. 124, p. 587.
10. R.A. Graham and D.M. Webb: in *Shock Waves in Condensed Matter*, Y.M. Gupta, ed., Plenum Press, New York, NY, 1986, pp. 831-36.
11. A.M. Staver: in *Shock Waves and High Strain Rate Phenomena in Metals*, M.A. Meyers and L.E. Murr, eds., Plenum Press, New York, NY, 1981, pp. 865-80.
12. R.A. Prümmer: in *Explosive Welding, Forming and Compaction*, T.Z. Blazynsky, ed., Applied Science Publishers, Ltd., London, 1983, pp. 369-95.